The Astrophysical Journal, 846:164 (9pp), 2017 September 10 https://doi.org/10.3847/1538-4357/aa85e2

Current and Future Constraints on Primordial Magnetic Fields

Dylan R. Sutton[1], Chang Feng[2], and Christian L. Reichardt[1]
[1] School of Physics, University of Melbourne, Parkville, VIC 3010, Australia; christian.reichardt@unimelb.edu.au
[2] Department of Physics and Astronomy, University of California, Irvine, CA 92697-4575, USA
Received 2017 February 6; revised 2017 August 9; accepted 2017 August 9; published 2017 September 13

Abstract

We present new limits on the amplitude of potential primordial magnetic fields (PMFs) using temperature and polarization measurements of the cosmic microwave background (CMB) from *Planck*, the BICEP2/Keck Array, POLARBEAR, and SPTpol. We reduce twofold the 95% confidence upper limit on the CMB anisotropy power due to a nearly scale-invariant PMF, with an allowed B-mode power at $\ell = 1500$ of $D^{\rm BB}_{\ell=1500} < 0.071\ \mu K^2$ for *Planck* versus $D^{\rm BB}_{\ell=1500} < 0.034\ \mu K^2$ for the combined data set. We also forecast the expected limits from soon-to-deploy CMB experiments (like SPT-3G, Adv. ACTpol, or the Simons Array) and the proposed CMB-S4 experiment. Future CMB experiments should dramatically reduce the current uncertainties by one order of magnitude for the near-term experiments and two orders of magnitude for the CMB-S4 experiment. The constraints from CMB-S4 have the potential to rule out much of the parameter space for PMFs.

Key words: cosmic background radiation – early universe – magnetic fields – polarization

1. Introduction

Measurements of the cosmic microwave background (CMB) temperature anisotropy have provided some of the most powerful tests of cosmology. We are now entering a new era as experiments begin to measure polarized "B-modes" in the CMB for the first time (Hanson et al. 2013; Ade et al. 2014; The POLARBEAR Collaboration, Ade et al. 2014; Naess et al. 2014; Keisler et al. 2015; Keck Array & BICEP2 Collaborations, Ade et al. 2016; Louis et al. 2016). Precision measurements of CMB polarization promise new tests of the standard cosmological model. The best known of these tests are searches for inflationary gravitational waves in B-modes at large angular scales and plans to measure the sum of the neutrino masses through the lensing B-modes on small angular scales (for a recent review, see Abazajian et al. 2016).

CMB B-mode measurements can also be used to constrain more exotic models, such as the possible existence of cosmic birefringence (Carroll 1998; Lue et al. 1999) or primordial magnetic fields (PMFs) (Kosowsky & Loeb 1996; Seshadri & Subramanian 2001). Both effects lead to the rotation of E-modes into B-modes, thereby increasing the amplitude of the BB power spectrum. By equating the magnitude of the resulting B-modes, parity-violating processes can be translated into an equivalent PMF strength. It is therefore common to simply quote effective limits on PMFs. In this work, we present new upper limits from current CMB polarization data on the possibility of PMFs or parity-violating physics.

Magnetic fields are ubiquitous in astronomy and are found almost universally in collapsed objects from stars to galaxies and galaxy clusters (for a review, see Ryu et al. 2012; Widrow et al. 2012). There is even some evidence for magnetic fields in intergalactic space from *Fermi*-LAT data (Neronov & Vovk 2010). High-energy γ-rays from blazars should produce electron–positron pairs when the γ-rays collide with infrared or optical photons. These pairs should later annihilate at GeV energies, but the expected GeV flux is missing in the *Fermi*-LAT observations. The missing flux could be explained by the deflection of particles due to intergalactic magnetic fields. There are, however, alternative explanations involving instabilities in the electron–positron plasma, leading pairs to deposit their energy in the intergalactic medium in the form of heat (Broderick et al. 2012). If the loss of flux is indeed due to magnetic fields, then the GeV results set lower limits on the intergalactic magnetic field strength of 10^{-9}–10^{-6} nG (Tavecchio et al. 2010; Dermer et al. 2011; Taylor et al. 2011; Vovk et al. 2012).

The mechanism to create large-scale magnetic fields, especially in intergalactic space, remains unclear. One popular proposal is that the observed fields are the product of PMFs, which are predicted by several theories of the early universe (e.g., Grasso & Riotto 1998; Turner & Widrow 1988; Ichiki et al. 2006). Adiabatic compression and turbulent shocks during later structure formation amplify these initial seed PMFs into the stronger magnetic fields observed today. Of course, this amplification process may be seeded through other means, such as active galactic nuclei or galactic dynamos (for a review, see Giovannini 2004). However, the possibility of PMFs opens up the intriguing idea that observations of large-scale magnetic fields may offer insights into the physics of the very early universe.

PMFs would have observational consequences for big bang nucleosynthesis (e.g., Kahniashvili et al. 2010), large-scale structure (e.g., Battaner et al. 1997), the ionization history of the universe (Kunze & Komatsu 2015), and the blackbody spectrum of the CMB (e.g., Kunze & Komatsu 2014), as well as the CMB anisotropies. The CMB anisotropies have yielded some of the strongest constraints on PMFs and are the focus of this work. There have been three recent results of note. Planck Collaboration et al. (2016) have used the *Planck* 2015 release of temperature and polarization data to set limits on a variety of PMF models. With the CMB power spectrum data that will be the focus of this paper, Planck Collaboration et al. (2016) find 95% confidence upper limits ranging from $B_{1\rm Mpc} < 5.6$ nG to <0.7 nG depending on the exact model. Here $B_{1\rm Mpc}$ is the rms magnetic field strength on a 1 Mpc length scale. The POLARBEAR collaboration also recently announced limits on PMFs from the POLARBEAR data using either a four-point estimator or B-mode power spectrum measurement (Ade et al. 2015). The strongest constraints were from the B-mode

spectrum; the observed upper limit was $B_{1\mathrm{Mpc}} < 3.9$ nG. Two other experiments, SPTpol and BICEP2/Keck Array, have also reported B-mode power spectrum measurements (Keisler et al. 2015; Keck Array & BICEP2 Collaborations, Ade et al. 2016), and Zucca et al. (2016) reported constraints from the combination of the *Planck* and SPTpol bandpowers. In this paper, we will combine the data from all four experiments to determine upper limits on PMFs, and find that the BICEP2/Keck Array data in particular improves these upper limits. We then present Fisher matrix forecasts on PMF models for the stage-III and stage-IV CMB experiments currently being built or designed.

The outline of this paper is as follows. In Section 2, we lay out the data and how we use them to put limits on PMFs. We present the results of this analysis on current data in Section 3. In Section 4, we forecast constraints from future experiments using a Fisher matrix formulism. We conclude in Section 5.

2. Data and Methods

We use Markov chain Monte Carlo (MCMC) methods to study constraints on PMFs. In this section, we first describe the CMB temperature and polarization anisotropy data used, and then discuss the MCMC implementation.

2.1. Data

We use a compendium of current measurements of the CMB temperature and polarization anisotropies from ground-based and satellite experiments. We use *Planck* data from the 2015 release to constrain the TT, TE, EE, and lensing power spectra. Specifically, these are the "plik_dx11dr21_HM_v18_TT," "lowTEB," and "lensing" *Planck* likelihood modules.

In addition to the *Planck* data, we use a number of ground-based CMB B-mode polarization measurements. First, we include measurements of the TE, EE, and BB power spectra from the SPTpol experiment (Crites et al. 2015; Keisler et al. 2015). The BB bandpowers cover the angular multipoles $\ell \in [500, 2000]$. We also add the BB bandpowers from POLARBEAR that cover the multipoles from 500 to 2500 (Ade et al. 2015). At these angular scales, both the SPTpol and POLARBEAR bandpowers primarily constrain the vector modes of a PMF. Finally, we include the latest BICEP2 and Keck Array joint analysis (Keck Array & BICEP2 Collaborations, Ade et al. 2016). This last data set also places limits on the tensor modes of a PMF due to its coverage of lower multipoles. During the writing of this paper, ACTpol polarization power spectra became available (Naess et al. 2014; Louis et al. 2016). We have not included them as the public likelihoods do not include the B-mode power spectrum; we do not expect adding the ACTpol bandpowers to significantly change the PMF limits based on a visual comparison of the current BB bandpowers from different experiments (see Figure 1). In all chains, we marginalize over the recommended foreground models for each data set. We do not, however, require consistency between these foreground models as the data do not have identical flux cuts for extragalactic sources and so on. These data are plotted against the expected B-mode power spectrum for the standard cosmological model in Figure 1.

2.2. Methods

We use MCMC methods to determine the parameter constraints reported in this work. The results are calculated

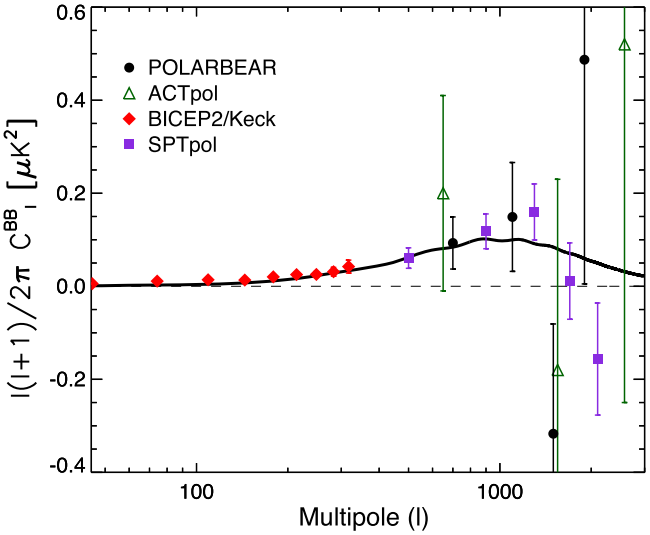

Figure 1. Current measurements of the CMB B-mode power spectrum. The black line shows the expected B-mode power spectrum in the *Planck* best-fit ΛCDM cosmology (with the tensor-to-scalar ratio r set to 0.01). The data sets are from POLARBEAR (black circles; the POLARBEAR Collaboration, Ade et al. 2014); ACTpol (dark green triangles; Naess et al. 2014); BICEP2/Keck Array (red diamonds; Keck Array & BICEP2 Collaborations, Ade et al. 2016); and SPTpol (purple squares; Keisler et al. 2015). The B-mode measurements used for the limits in this work are denoted with filled symbols. Current B-mode measurements are noise-limited at all angular multipoles; the next generation of experiments will significantly increase the signal-to-noise on the B-mode power spectrum.

using the CosmoMC[3] package (Lewis & Bridle 2002). CosmoMC invokes CAMB[4] (Lewis et al. 2000) to calculate the CMB power spectrum for each set of cosmological parameters. Although CosmoMC and CAMB have a partial implementation of PMFs, we choose to adopt a simpler, fast, template-based calculation for the PMF-sourced power. We have adapted CosmoMC to add a scaled version of a PMF template to all four CMB power spectra: TT, TE, EE, and BB, where the scale factor is A_{PMF}:

$$C_\ell = C_\ell^{\mathrm{CAMB}} + A_{\mathrm{PMF}}\left[C_\ell^{\mathrm{PMF,vec}} + \left(\frac{\beta}{20}\right)^{1.9} C_\ell^{\mathrm{PMF,tens}}\right]. \quad (1)$$

The calculation of the PMF templates, $C_\ell^{\mathrm{PMF,vec}}$ and $C_\ell^{\mathrm{PMF,tens}}$, and the motivation for the β scaling are described in Section 2.3. The parameter $\beta = \ln(a_\nu/a_{\mathrm{PMF}})$ relates the timing of neutrino decoupling and the generation of the PMF, where a_x represents the scale factor at the respective events. Note that no other effect of PMFs is considered; this is one reason why we only use CMB data.

For the real data, unless noted, we assume the six-parameter, spatially flat ΛCDM model with a single massive neutrino of 60 meV and two parameters, A_{PMF} and β, describing the power due to PMFs. We adopt flat priors on all parameters. There are two points to note about the PMF priors. First, this is a flat prior on the observed PMF power, A_{PMF}, not the rms magnetic field strength, $B_{1\mathrm{Mpc}}$, that has often been used in the literature. In the current era of upper limits, this prior choice has some impact on the resulting PMF limits. Second, the exact range of the uniform prior on β matters. Here we follow Planck

[3] http://cosmologist.info/cosmomc (2015 July version).
[4] http://camb.info

Collaboration et al. (2016) and Zucca et al. (2016) and use $\beta \in [11.513, 41.447]$.[5] However, the constraints, especially those from *Planck* alone, weaken substantially if the lower bound on β is lowered further. If we follow Ade et al. (2015) who used $\beta \in [0, 39]$, the upper limits are relaxed by a factor of roughly eight for *Planck*-only and by a factor of two for the combined data set. We sometimes also add $A_{\rm lens}$ as a simple way of marginalizing over uncertainty in the predicted lensed BB power spectrum for any extension to the ΛCDM model. Finally, we sometimes allow non-zero tensors, parameterized by the tensor-to-scalar ratio, r.

2.3. Primordial Magnetic Field Template

The density and stress perturbations introduced by PMFs give rise to vorticity and gravitational waves in the early photon–baryon plasma, i.e., vector and tensor modes, as well as scalar modes. The exact amplitude of these modes can be calculated by modifying the normal Boltzmann equations to include sources due to the PMFs. The primary PMF anisotropy is assumed to be Gaussian distributed with a power-law power spectrum, $A_{\rm B}k^{n_{\rm B}}$, where $n_{\rm B}$ is the spectral index and $A_{\rm B}$ is the PMF power normalization. We can translate the normalization, $A_{\rm B}$, into more physically motivated units by calculating the rms of the PMF field strength over a length scale of 1 Mpc, which we will call $B_{\rm 1Mpc}$. Finally, the timing of when PMFs are generated relative to neutrino decoupling matters for the tensor component because the PMF-induced stress anisotropy can be compensated for by decoupled or partially decoupled neutrinos. The timing is parameterized by $\beta = \ln(a_\nu/a_{\rm PMF})$, the natural logarithm of the ratio of the scale factors at neutrino decoupling and PMF generation.

Given that we are still in the era of upper limits, we fix the value of $n_{\rm B}$ instead of exploring the full three-dimensional PMF parameter space. For the real data, we focus on a nearly scale-invariant ($n_{\rm B} = -2.9$) PMF template in this work due to its connection to inflation. Quantum mechanical zero-point fluctuations during inflation can generate an approximately scale-invariant PMF with a spectral index close to $n_{\rm B} = -3$ (e.g., Turner & Widrow 1988; Mack et al. 2002; Kahniashvili et al. 2008). In contrast, causal PMFs with bluer spectra require later phase transitions or other new physics after inflation (e.g., Durrer & Caprini 2003; Subramanian 2016). We also consider $n_{\rm B} = -1$ and $n_{\rm B} = 2$ for the forecasts in Section 4. For each value of $n_{\rm B}$, we use publicly released modifications to CAMB from Zucca et al. (2016) to calculate a PMF template for the CMB TT, TE, EE, and BB power spectra at fixed parameters: $B_{\rm 1Mpc} = 2.5$ nG and $\beta = 20.72$ ($a_\nu/a_{\rm PMF} = 10^9$). The calculated templates include tensor and vector PMF contributions; scalar contributions are not implemented. The lack of scalar terms should not matter for CMB polarization data. Temperature data are not the main focus of this work, and we find our *Planck* results to be consistent with Planck Collaboration et al. (2016), suggesting the impact of the scalar terms is minor. The PMF templates are plotted against other signals in the CMB B-mode power spectrum in Figure 2 and against each other in Figure 3.

As noted in the previous section, the MCMC includes a scaling parameter, $A_{\rm PMF}$, for the PMF power spectrum template. We can translate the amplitude constraint on this template to a constraint on the rms magnetic field strength on

[5] This corresponds to $\log_{10}(a_\nu/a_{\rm PMF}) \in [4, 17]$.

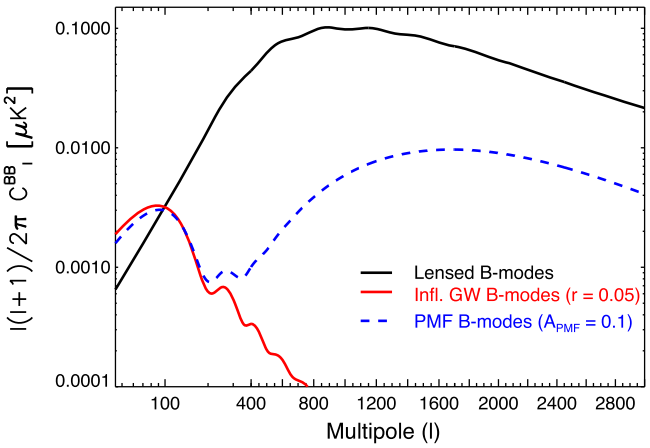

Figure 2. Expected sources of CMB B-modes. The black line shows the expected lensing B-mode power in the *Planck* best-fit ΛCDM cosmology, while the red line corresponds to the B-modes due to inflationary gravitational waves for $r = 0.05$. The dashed blue line shows the nearly scale-invariant ($n_{\rm B} = -2.9$) PMF template used in this work, scaled to $A_{\rm PMF} = 0.2$ (i.e., $B_{\rm 1Mpc} = 1.7$ nG) to match the gravitational wave signal. At $\ell < 200$, the tensor contribution from PMFs closely resembles the expected inflationary gravitational wave signal, and the two signals are effectively degenerate on these angular scales in a power spectrum (two-point) analysis.

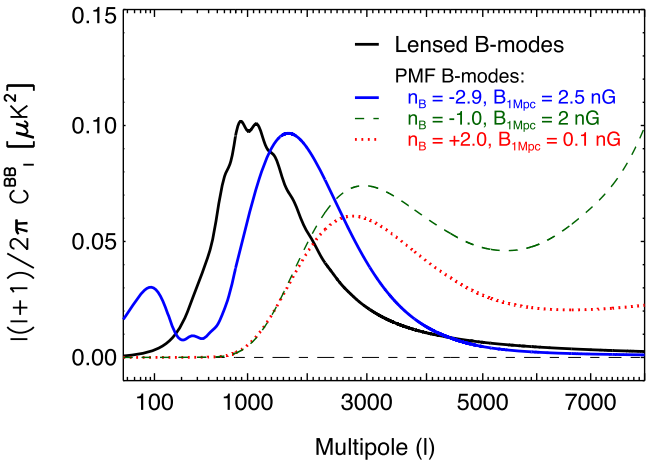

Figure 3. How the expected B-mode power due to PMFs changes with the spectral index, $n_{\rm B}$. The lensing B-mode power spectrum (solid, black line) is plotted against the PMF power for $n_{\rm B} = -2.9$ (solid blue line), $n_{\rm B} = -1$ (dashed green line), and $n_{\rm B} = +2$ (dotted red line). To keep all the curves on the same scale, we adjust the rms strength of the magnetic field, $B_{\rm 1Mpc}$, between the three cases as noted in the legend. For a fixed rms magnetic field strength, increasing $n_{\rm B}$ greatly increases the expected B-mode power. There is an inflection point between the nearly scale-invariant PMF with $n_{\rm B} = -2.9$ and the bluer PMF spectra ($n_{\rm B} = -1$ or 2) which shifts power to smaller angular scales and eliminates the peak at $\ell \lesssim 200$.

1 Mpc scales, $B_{\rm 1Mpc}$, using the expected scaling:

$$C_\ell^{\rm vec} \propto B_{\rm 1Mpc}^4. \quad (2)$$

An unfortunate consequence of this steep fourth-power scaling is that substantial reductions in the observationally allowed power lead to only modestly better limits on the magnetic field strength. However, if a PMF is detected, the steep scaling between $B_{\rm 1Mpc}$ and the observed CMB B-mode power spectrum would allow excellent constraints on the PMF properties.

The power in the tensor modes also depends on the timing of PMF generation relative to neutrino decoupling, and is expected to scale approximately as β^2 (Lewis 2004; Shaw &

Table 1
Parameter Constraints

Model	$A_{\rm PMF}$	$A_{\rm lens}$	r
ΛCDM			
+ $A_{\rm PMF}$	<0.36	⋯	⋯
+ $A_{\rm PMF}$ + $A_{\rm lens}$	<0.30	1.123 ± 0.064	⋯
+ $A_{\rm PMF}$ + $A_{\rm lens}$ + r	<0.25	1.127 ± 0.063	<0.07

Note. In the minimal model, ΛCDM + $A_{\rm PMF}$, current CMB power spectra data from *Planck*, POLARBEAR, SPTpol, and BICEP2/Keck Array place a 95% confidence upper limit on the PMF power of $A_{\rm PMF} < 0.36$. This limit tightens slightly if tensor modes (r) are allowed, or the amount of lensing is allowed to vary. In the case of r, the tightening is because the observed power at large angular scales is now split between PMFs and inflationary gravitational waves. In the case of $A_{\rm lens}$, it is because the preferred value for $A_{\rm lens}$ is modestly above the predicted value of unity. Recall that the the PMF template is normalized to unity for $B_{\rm 1Mpc} = 2.5$ nG.

Lewis 2010). We double-check this expectation for β in the range 2 to 20 using the Zucca et al. (2016) code, and find the computed tensor power scales as $\beta^{1.9}$ We use this β power-law form to handle the PMF timing dependence. Thus, the tensor PMF power will scale as

$$A_{\rm PMF}^{\rm tens} \propto B_{\rm 1Mpc}^4 \beta^{1.9}. \quad (3)$$

3. Results

We begin by investigating how the addition of ground-based CMB polarization data to *Planck* data affects the limits on PMFs. For the real data, we focus on the most theoretically motivated scenario of an approximately scale-invariant spectrum for the PMFs ($n_{\rm B} = -2.9$), although we will consider other scenarios in the forecasts of the next section. The ground-based CMB polarization data substantially reduce the allowed PMF power; we see a factor of two reduction over *Planck* alone in the simple eight-parameter model. The 95% confidence upper limit for *Planck* is $A_{\rm PMF} < 0.76$ for ΛCDM + PMF. Adding the ground-based experiments brings this limit to $A_{\rm PMF} < 0.36$. To facilitate a physical interpretation, we can restate these limits as an allowed B-mode power at $\ell = 1500$, which is near the peak of the PMF contribution. The equivalent limits on the allowed B-mode power are $D_{\ell=1500}^{\rm BB} < 0.071\ \mu K^2$ for *Planck*alone and $D_{\ell=1500}^{\rm BB} < 0.034\ \mu K^2$ when the ground-based experiments are added. We test which data sets are important by adding single data sets to the *Planck* data, and find that the source of the improvement is evenly split between SPTpol and BICEP2/Keck Array. Adding either one to *Planck* yields the same 95% confidence upper limit: $A_{\rm PMF}^{\rm Planck+BICEP2/KeckArray} < 0.44$ versus $A_{\rm PMF}^{\rm Planck+SPTpol}) < 0.45$. Extending the β prior to lower values would shift the relative weight more toward SPTpol (and vice -versa). Similarly, increasing the value of $n_{\rm B}$ would increase the relative importance of the smaller angular scales measured by SPTpol. In short, the source of the factor of two reduction in the upper limit on $A_{\rm PMF}$ for a nearly scale-invariant PMF spectrum ($n_{\rm B} = -2.9$) is due to a more accurate measurement of the B-mode power spectrum at all scales.

We next look at the model dependence of these upper limits. We list the limits for the combined data set with different parameter sets in Table 1. First, we vary the largest source of B-mode power, gravitational lensing, by allowing $A_{\rm lens}$ to float. Somewhat counterintuitively, the limits are somewhat better with $A_{\rm lens}$ allowed to vary (this is due to a mild preference for $A_{\rm lens}$ above unity which increases the lensed B-mode power). In this case for *Planck* alone, the 95% confidence upper limit is $A_{\rm PMF} < 0.64$, dropping to $A_{\rm PMF} < 0.30$ with the ground-based experiments. Next we introduce inflationary gravitational waves, as parameterized by the tensor-to-scalar ratio r. The 95% confidence upper limit on $A_{\rm PMF}$ drops again. This is easily understood as a splitting of the large-scale B-mode power between two positive-definite terms: r and $A_{\rm PMF}$.

We also propagate the limits on the observed PMF power into limits on the magnetic field strength, $B_{\rm 1Mpc}$. We do this using the scaling of Equation (2), $A_{\rm PMF} \propto B_{\rm 1Mpc}^4$. Given this scaling, the observed upper limits with a flat prior on $A_{\rm PMF}$ would lead to an apparent "detection" of $B_{\rm 1Mpc}$. We therefore importance sample the chains to apply a flat prior on $B_{\rm 1Mpc}$. We find a 95% confidence upper limit of $B_{\rm 1Mpc} < 1.8$ nG for *Planck* alone, similar to the limit found by Planck Collaboration et al. (2016) of $B_{\rm 1Mpc} < 2.0$ nG with $n_{\rm B} = -2.9$ held fixed as we have done. Adding the ground-based polarization measurements significantly reduces the 95% confidence upper limit to $B_{\rm 1Mpc} < 0.91$ nG. Due to the inclusion of the BICEP2/Keck Array and POLARBEAR data, these results are slightly lower than the *Planck* + SPTpol upper limit of <1.2 nG quoted by Zucca et al. (2016).

4. Forecasts

The sensitivity of CMB experiments is increasing rapidly due to the continued growth in the number of detectors. Abazajian et al. (2016) thus defines four stages of CMB experiments. Current experiments are called stage II. The B-mode measurements from these stage II experiments were used for PMF constraints in the previous section and are plotted in Figure 1. Stage III experiments such as SPT-3G, the Simons Array, or AdvACTPol (Benson et al. 2014; Henderson et al. 2016; Suzuki et al. 2016) have approximately ten times more detectors, and generically will start collecting data around 2017 and finish three to four years later. In this section, we forecast the expected constraints from the EE and BB power spectrum measurements of the stage III experiments by combining forecasts for SPT-3G and the Simons Array. There is also a proposal to build a stage IV experiment, CMB-S4, that would increase the detector counts by another order of magnitude and should begin taking data in the early 2020s. A pathfinder to CMB-S4, the Simons Observatory, was funded in 2016. We examine the likely PMF constraints from the EE and BB power spectrum measurements with CMB-S4, and look at how to design CMB-S4 to maximize its potential for PMF searches.

4.1. Methods and Experimental Parameters

We use Fisher matrices to forecast the potential constraints on PMFs possible for each generation of experiments. The Fisher matrix, $\mathcal{F}_{ij}$, can be defined as

$$\mathcal{F}_{ij} = \frac{1}{2}\frac{\partial^2 \chi^2}{\partial p_i \partial p_j}, \quad (4)$$

for model parameters $\boldsymbol{p}$. The inverse of the Fisher matrix is the covariance matrix of the parameters for Gaussian likelihoods. While Fisher matrices can underestimate the true uncertainties for non-Gaussian likelihoods (see, e.g., Wolz et al. 2012), they

Table 2
Assumed Survey Parameters

Experiment	Sky Coverage	Polarized Noise Level (μK arcmin)	$1/f$ Knee	Beam FWHM (arcmin.)
CMB Stage III				
SPT-3G	6%	3.0	200	1.2
Simons Array	36%	9.5	200	3.5
CMB Stage IV	55%	1.3	100	4.0

Note. Key numbers about the planned stage III and IV experiments. The sky coverage percentages are after galactic cuts. Unless otherwise noted, the Fisher matrix forecasts in this work use these numbers. All forecasts also allow for beam and calibration uncertainties as noted in the text.

make it easy to combine information from different experiments and estimate the final parameter constraints.

We include two external data sets in all forecasts. The first data set is the expected measurements of the TT, TE, and EE spectra from the *Planck* satellite. We include *Planck* TT information in the multipole range $2 \leqslant \ell \leqslant 3000$. Due to the importance of galactic foreground removal at large scales in polarization, we only use TE and EE information starting from $\ell = 30$. A prior on the optical depth of 0.005 is added to account for the optical depth constraint expected from the missing multipoles. Second, we include a 1% external measurement of the Hubble constant, such as is expected from the Taipan experiment (Kuehn et al. 2014).

To calculate the Fisher matrix for a CMB experiment, we need the bandpower covariance matrix and partial derivatives of the CMB spectra. The partial derivatives are calculated numerically from CAMB spectra (Lewis et al. 2000). We calculate the bandpower covariance matrix using the Knox formula (Knox 1997) for the survey parameters in Table 2. The sample variance contribution is calculated assuming the *Planck* best-fit ΛCDM cosmology with a small gravitational wave contribution ($r = 0.01$) added. This is the black line in Figure 1. We use a bandpower bin size of $\Delta\ell = 50$. We assume a 5% uncertainty on the beam FWHM and a 1% power calibration uncertainty. In Section 4.3.5, we test relaxing or tightening the beam and calibration uncertainty and find the beam and calibration uncertainties have a negligible impact on the PMF constraints.

One concern with combining Fisher matrices from different experiments is double-counting modes due to overlapping sky coverage. We avoid this problem in different ways in each of the CMB power spectra. For the TT and TE spectra, we only use the *Planck* measurements. We do not expect future experiments to substantially improve upon *Planck* in these spectra which are already cosmic variance limited out to fairly high multipoles. We do the opposite for the EE and BB spectra. We do not include *Planck* BB information in any forecast, and we discard *Planck* EE data in the overlap region by appropriately scaling the *Planck* EE uncertainties. We ignore overlaps between the stage III experiments on the basis that the sky overlap between a Chilean experiment like the Simons Array and South Pole experiment like SPT-3G will be small. The overlap issue is also the rationale behind using only one of the Simons Array and AdvACTpol as the two experiments are likely to have substantial sky overlap. The overlap in sky coverage will almost certainly be substantial between stage III and IV experiments; thus we do not include the stage III experiments, except as a prior on the polarized Poisson power, in the CMB-S4 constraints. This prior is only relevant in practice when the assumed CMB-S4 configuration has a larger beam size than SPT-3G. With these measures in place, this analysis should not double-count any modes.

We consider the constraints on PMFs in two cosmologies. Our fiducial cosmology is a 12-parameter model that extends ΛCDM with four commonly considered extensions as well as PMFs: $\Lambda\mathrm{CDM} + r + n_{\mathrm{run}} + N_{\mathrm{eff}} + \sum m_\nu + A_{\mathrm{PMF}} + \beta$. Here, n_{run} is running of the scalar index, N_{eff} is the effective number of relativistic species, and $\sum m_\nu$ is the sum of the neutrino species. This 12-parameter model is our default cosmological model when forecasting future PMF constraints as these extensions are all well-motivated theoretically. We have examined the degree to which A_{PMF} is degenerate with the 10 parameters unrelated to PMFs—the only strong degeneracy is in the $n_{\mathrm{B}} = -2.9$ case and is with r. The reason for this degeneracy is illustrated in Figure 2, which shows that the tensor mode power due to inflationary gravitational waves and a PMF with $n_{\mathrm{B}} = -2.9$ is nearly identical on large angular scales. To test the degree to which parameter degeneracies limit the inferred constraints, we also quote constraints from a "minimal" eight-parameter model in which the PMF power is the only extension to ΛCDM: $\Lambda\mathrm{CDM} + A_{\mathrm{PMF}} + \beta$. In both cases, we always marginalize over unknown Poisson EE and BB terms due to polarized extragalactic sources. We assume the galactic foregrounds are removed by a judicious combination of data from multiple frequencies.

In this work, we restrict ourselves to power spectrum (i.e., two-point estimators) searches for PMFs. Currently the power spectrum limits from *Planck* or POLARBEAR are better than the four-point upper limits. Although outside the scope of this work, it would be interesting to extend this analysis to four-point estimators in the future. First, the four-point limits should improve faster as the noise level falls. Second, in the case of a detection, the four-point estimators would almost certainly come into play to learn more about the vector modes of the PMFs. The detection (or non-detection) of the vector PMF signal in the four-point estimators could then be used to argue for whether it is more likely that any observed tensor power is due to inflationary gravitational waves or PMFs. Finally, a lensing estimator might be used to "de-lens" the B-mode power spectrum, thereby suppressing the lensed B-mode signal and allowing better limits on PMFs. Such de-lensing techniques have long been proposed for inflationary gravitational wave searches (e.g., Kesden et al. 2002; Knox & Song 2002; Seljak & Hirata 2004; Simard et al. 2015) and more recently been demonstrated on real *Planck* data (Larsen et al. 2016).

4.2. Stage III Forecasts

The experiments that will begin taking data in 2017 will dramatically improve our knowledge of PMFs. In the minimal cosmological model, the 1-σ forecast for *Planck*+H_0 is $\sigma(A_{\mathrm{PMF}}) = 0.38$ for a best-motivated, nearly scale-invariant PMF spectrum (i.e., $n_{\mathrm{B}} = -2.9$). We have set a Gaussian prior on β with σ_β chosen such that the Fisher forecast matches the actual upper limit from the *Planck* data. Adding EE and BB bandpowers from two stage III experiments, SPT-3G and Simons Array, reduces the uncertainty by more than an order of magnitude in the eight-parameter model to $\sigma(A_{\mathrm{PMF}}) = 0.020$. The relative improvement is larger in the more realistic 12-parameter model, as parameter degeneracies substantially

weaken (by a factor of five) the *Planck*+H_0 constraints on $A_{\rm PMF}$, while weakening the stage III constraint by a more modest 40%. Thus within the 12-parameter model, the addition of stage III CMB experiments improves the $A_{\rm PMF}$ uncertainty by a factor of $\sim$35 to $\sigma(A_{\rm PMF}) = 0.022$. The parameter degeneracies largely disappear for steeper PMF spectra (i.e., $n_{\rm B} = -1$ or 2) as the PMF B-mode spectra then peak at very small scales and this small-scale power cannot be mimicked by any of the other parameters. The improvement from adding the SPT-3G and Simons Array experiments to *Planck* remains impressive for these values of $n_{\rm B}$. For the 12-parameter model and $n_{\rm B} = -1$, adding SPT-3G and Simons Array to *Planck* leads to a 17-fold reduction in $\sigma(A_{\rm PMF})$ from 0.38 to 0.023. For $n_{\rm B} = 2$, there is a 20-fold reduction from $\sigma(A_{\rm PMF}) = 3.0 \times 10^{-6}$ to 1.5×10^{-7}. We can expect substantially tighter constraints on PMFs by the end of the decade.

4.3. Stage IV Forecasts

The primary motivations behind the proposed CMB-S4 experiment are to search for inflationary gravitational waves and to measure the neutrino masses. However, CMB-S4 would also enable extremely sensitive searches for PMFs. We begin by considering our fiducial CMB-S4 configuration, as laid out in Table 2. For this fiducial configuration and the 12-parameter cosmological model, we find a threefold reduction over the stage III experiments for all three PMF template shapes. The expected uncertainties for CMB-S4 are $\sigma(A_{\rm PMF}^{n_{\rm B}=-2.9}) = 6.3 \times 10^{-3}$, $\sigma(A_{\rm PMF}^{n_{\rm B}=-1}) = 7.4 \times 10^{-3}$, and $\sigma(A_{\rm PMF}^{n_{\rm B}=2}) = 5.2 \times 10^{-8}$. These represent more than a 50-fold improvement on current limits.

Given that CMB-S4 is being designed, it is worth considering how design decisions would affect the final PMF constraints. We look at five aspects of the experiment: the instrumental sensitivity (as reflected by the final noise level in the maps), the telescope size or beam FWHM, the low-ℓ noise performance, the amount of sky surveyed, and how well the beam shape and calibration must be known. Of these five aspects, we find the first two to be very important to PMF searches and the second two to be somewhat important. As might be expected, in some cases the optimal design depends on the shape of the PMF spectrum ($n_{\rm B}$) as this sets the relative power between large and small angular scales. However, as was discussed in Section 2.3, there are theoretical reasons to expect the PMF spectrum to be close to a scale-invariant spectrum. While for completeness we present results for three values of $n_{\rm B}$, we recommend favoring the optima for $n_{\rm B} = -2.9$.

4.3.1. Instrumental Sensitivity (Map Noise Levels)

Reducing the noise in CMB maps will monotonically improve power spectrum measurements. The goal of this section is to quantify the magnitude of that improvement: has the information gain saturated, or will further reductions in noise substantially improve PMF searches? Figure 4 shows the uncertainty on $A_{\rm PMF}$ as a function of the map noise level for the three PMF templates in either the 12- or eight-parameter cosmological models. For this figure, we have fixed the rest of the experimental configuration (i.e., everything except the polarized noise levels) to the values of the CMB-S4 row in Table 2. Clearly, continuing to improve the sensitivity of CMB experiments to CMB-S4 and beyond will be a major boon to PMF searches. In the general, 12-parameter cosmological model, the PMF uncertainty does not plateau in any of the three PMF templates considered until the map noise is at or below 0.3 μK arcmin (a factor of four lower than the fiducial CMB-S4 configuration).

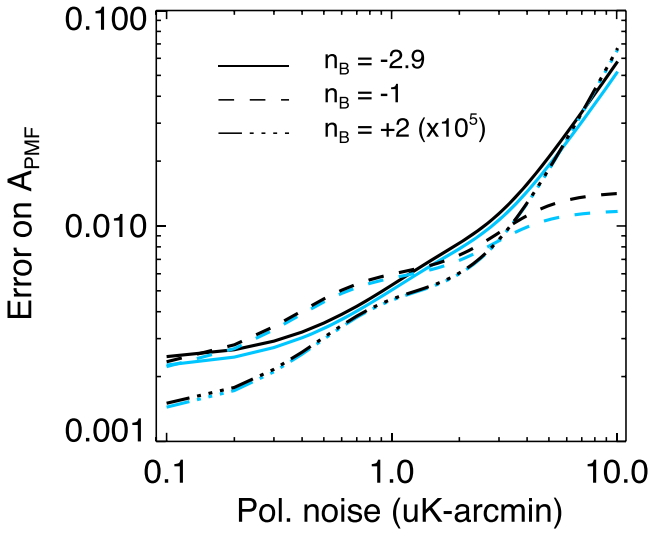

Figure 4. How the PMF uncertainty scales with the polarized map noise. Forecasts are shown as a function of the map noise in μK arcmin for each of the three PMF spectral indices: $n_{\rm B} = -2.9$ (solid), -1 (dashed), and $+2$ (dashed–dotted). In the case of $n_{\rm B} = 2$, the uncertainties have been multiplied by a factor of 10^5 to allow them to be plotted on the same scale. The black lines are for the fiducial 12-parameter model, while the light blue lines are for the minimal ΛCDM + $A_{\rm PMF}$ model. The model only matters in the nearly scale-invariant PMF case, where the constraints degrade in the 12-parameter model due to a degeneracy with the tensor-to-scalar ratio. The PMF constraints improve rapidly with lower noise levels in all six cases up to $\sim$1 μK arcmin, which is close to the fiducial CMB-S4 noise levels.

4.3.2. Size of Telescope

Larger telescopes can recover more modes on the sky, and should therefore always improve the PMF constraints. As shown in Figure 5, we find the gains due to resolution at fixed mapping speed to be substantial for all three power-law indices considered. We see a local plateau between FWHMs of 4′ to 6′; improving the angular resolution in this range does little to aid PMF searches. We can understand this plateau by looking on the predicted PMF power in Figure 3. All three templates have two peaks across this range of angular multiples, and we would expect to see such a plateau when, for instance, the resolution is adequate to resolve the first peak, but not yet sufficient to resolve the second peak. The observed plateau positions are consistent with this hypothesis. Overall, a beam size of FWHM = 1′ instead of 10′ reduces the expected upper limit fivefold for $n_{\rm B} = -2.9$ and 30- to 35-fold for the steeper PMF indices which are more heavily weighted toward small angular scales. The model only matters in the nearly scale invariant PMF case ($n_{\rm B} = -2.9$), where the information on large angular scales dominates and the telescope size is relatively unimportant.

However, larger telescopes are also more expensive to build, which means for a fixed experimental budget, they would necessitate less ambitious focal planes and lower instantaneous mapping speeds. We very crudely approximated a cost-neutral setup with a noise level of 1.3 μK arcmin for a FWHM of 4′, a noise level of 2.8 μK arcmin for a FWHM of 2′, and a noise level of 4.0 μK arcmin for a FWHM of 1′. We find that

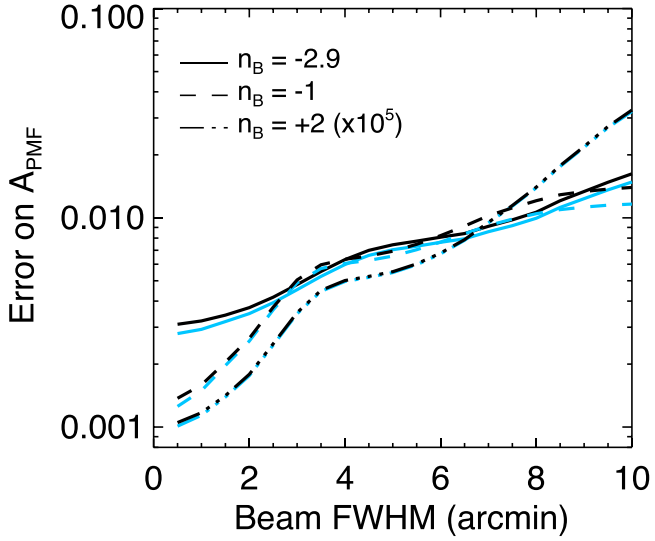

Figure 5. Larger telescopes (and thus smaller beams) improve limits on the PMF power. Forecasts are shown as a function of the beam FWHM in arcminutes for each of the three PMF scalar indices: $n_B = -2.9$ (solid), -1 (dashed), and $+2$ (dashed–dotted). In the $n_B = 2$ case, the uncertainties have been multiplied by a factor of 10^5 for plotting purposes. The black lines are for the fiducial 12-parameter model, while the light blue lines are for the minimal ΛCDM + A_{PMF} model. The cosmological model only matters in the nearly scale-invariant PMF case ($n_B = -2.9$), where the information on large angular scales dominates and the telescope size becomes less important. The plateau near $4'$ for $n_B = -1, +2$ is where the gain from the $\ell \sim 3000$ peak is saturated, but the resolution is not yet adequate to pick up the next peak at $\ell > 8000$ (see Figure 3).

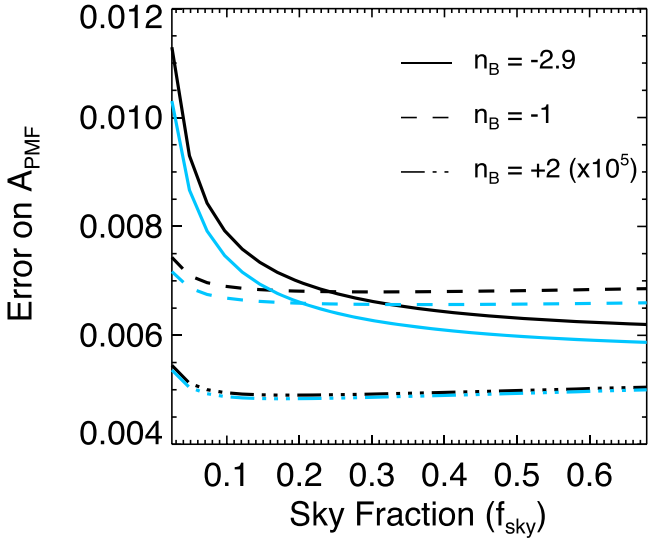

Figure 6. Dependence of preferred survey area for PMF searches on the PMF spectral index. In the best-motivated, nearly scale-invariant $n_B = -2.9$ case (solid line), we find PMF searches should observe more than $\sim$15%. In contrast, for the cases where $n_B = -1, +2$ (dashed and dot-dashed lines), we find that observing $\sim$10% of the sky produces the best PMF constraints. Note that in the case of $n_B = 2$, the uncertainties have been multiplied by a factor of 10^5 for plotting purposes. There is essentially no difference to the preferred areas between the 12-parameter cosmological model (black) or the restricted ΛCDM + PMF eight-parameter model (light blue). Fortunately, the minima for all three templates are relatively broad, and a survey covering 15+% of the sky will do well for all values of the PMF spectral index.

improving the mapping speed rather than telescope size leads to somewhat better potential limits for these experimental configurations, by a factor of 1.6, 1.1, or 1.1 for $n_B = -2.9$, -1, $+2$ respectively. However the results are close enough that the crudeness of the cost-neutral estimates used here is a worry, and the preference might flip for more accurately costed setups. In short, the tradeoff between larger telescopes or more detectors is largely a wash, although one might lean toward adding more detectors.

4.3.3. Survey Area

A third question is how much sky to observe with CMB-S4. Unsurprisingly, we find opposing preferences for the nearly scale-invariant $n_B = -2.9$ (which peaks at large angular scales) and the bluer $n_B = -1$ or 2 spectra which peak at smaller scales. As shown in Figure 6, observing at least 15% of the sky is very important to a search for nearly scale-invariant PMFs, and it is best to cover as much sky as possible. A caveat to this analysis is that it is likely easier to remove galactic foregrounds to a specified level on targeted, "clean" patches as opposed to a substantial fraction of the sky, and we would expect galactic foregrounds to be important for the large angular scales. That said, the PMF constraints improve by a factor of 1.4–1.5 (depending on the cosmological model) going from 10% to 25% of the full sky, and are nearly flat (a 6% improvement) from 25% to 70% of the sky (the widest area likely to be possible after galactic cuts). Conversely for $n_B = -1$ or $+2$, the optimal survey area is around 15% of the full sky. Note, however, that the minimum is extremely broad with only a 10% worsening of the expected uncertainty as the survey area is increased from 10% to 70% of the full sky. A survey covering at least 25% of the sky would perform well for all three considered PMF models.

4.3.4. Noise Performance at Large Angular Scales

Next we turn to the recovery of large angular scales on the sky, and the required noise performance at these low frequencies. For this, we look at the impact of shifting the $1/f$ knee of the map-space noise. Specifically, we are multiplying the noise power, N_ℓ, which is a constant for white noise, by a function of angular multipole:

$$f(\ell) = 1 + \left(\frac{\ell_{\rm knee}}{\ell}\right)^{8/3}. \quad (5)$$

The exponent, $8/3$, was selected based on a Kolmogorov spectrum of turbulence within a thin plane (Lay & Halverson 2000). Note that this knob serves as a placeholder for several effects, including a signal-to-noise hit due to galactic foregrounds or the methods used to clean these foregrounds, atmospheric noise, or actual instrumental low-frequency noise.

We generally find the forecasts to be insensitive to the $1/f$ knee or galactic foreground removal at the default beam size of $4'$. As Shown in Figure 7, it appears that even in the nearly scale-invariant case, the PMF constraint is coming primarily from smaller angular scales due to the degeneracy at large angular scales with both the tensor-to-scalar ratio and the PMF timing parameter β. For the bluer PMF spectra ($n_B = -1$ or 2), the forecasts show no dependence on the knee frequency. For the fiducial 12-parameter model, our ability to separate a PMF from other physics is coming from sub-degree angular scales.

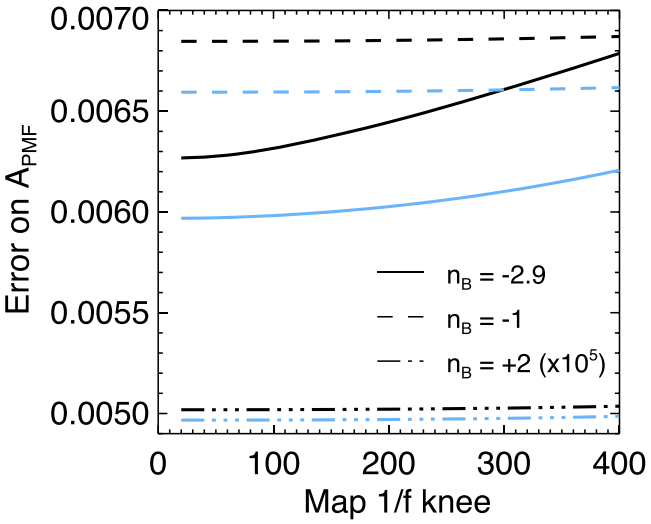

Figure 7. Recovering large angular scales is only important for a nearly scale-invariant PMF ($n_B = -2.9$) in the restricted ΛCDM + PMF eight-parameter model (solid, light blue line). The achieved map $1/f$ knee frequency makes no difference to CMB-S4 PMF searches in the 12-parameter model (black lines). For $n_B = -2.9$, this transition occurs because the 12-parameter model introduces a degeneracy with r on the large angular scales impacted by the map $1/f$ knee. The $1/f$ knee frequency also makes no difference for the bluer PMF templates (dashed and dashed–dotted black lines) in either the restricted (light blue) or full 12-parameter (black) model space. Note that in the case of $n_B = 2$, the forecasts have been multiplied by a factor of 10^5 for plotting purposes.

The low-frequency noise performance of CMB-S4 is not crucial to PMF searches.

4.3.5. Beam and Calibration Uncertainties

Finally, we consider whether searches for PMFs introduce new requirements on the accuracy to which the beam or calibration of an experiment must be known. We find they do not. We parameterize the beam uncertainty as a fractional uncertainty on the FWHM of a Gaussian beam, and calibration uncertainty as an overall power uncertainty. We find negligible, sub-percent shifts in the forecasted PMF uncertainties for calibration uncertainties from 0.2% to 5% and beam FWHM uncertainties from 2% to 12.5%. The PMF constraints for all three power-law indices considered are insensitive to the beam and calibration uncertainties.

5. Conclusions

In this work, we have improved the current upper limits on the strength of primordial magnetic fields by including more CMB B-mode polarization data. By adding BICEP2/Keck Array, POLARBEAR, and SPTpol to *Planck* data we have found that the 95% confidence upper limit on the PMF power falls nearly twofold from $A_{PMF} < 0.76$ to $A_{PMF} < 0.36$. The two major contributors to this improvement are the low-ℓ B-mode data from BICEP2/Keck Array and the high-ℓ B-mode data from SPTpol.

We have also shown that the next generation of experiments should dramatically reduce these limits, with the potential to detect PMFs for the first time. The so-called stage III experiments, which will begin taking data in 2017, can be expected to set upper limits at the level of $A_{PMF} < 0.02$ even after marginalizing over a six-parameter extension to ΛCDM and foregrounds.

The potential for detection increases even further with planned experiments like the Simons Observatory or CMB-S4. We have shown that an ideal version of CMB-S4 might decrease the 95% confidence upper limits eightfold, to $A_{PMF} < 0.0025$, and more realistic versions can still set upper limits on order of $A_{PMF} < 0.006$ in a 12-parameter cosmological model with $\Lambda\mathrm{CDM} + r + n_{run} + N_{eff} + \sum m_\nu + A_{PMF} + \beta$. This represents a threefold improvement over the forecasts for the stage III experiments and a more than 100-fold improvement over the current limits for this cosmological model. We have considered how the design of future experiments will impact the resulting PMF limits, looking at the experimental sensitivity, angular resolution, survey area, low-frequency noise performance, and beam or calibration uncertainties. We have found an experiment's sensitivity followed by telescope size to be the most important factors in predicting the PMF limits. CMB-S4 will be a very exciting probe of PMFs and other sources of cosmic birefringence.

We thank the referee as well as Srinivasan Raghunathan and Federico Bianchini for valuable feedback on the manuscript. C.R. is the recipient of an Australian Research Council Future Fellowship (FT150100074), and also acknowledges support from the University of Melbourne. C.F. acknowledges support from NASA grants NASA NNX16AJ69G and NASA NNX16AF39G. This research used resources of the National Energy Research Scientific Computing Center, which is supported by the Office of Science of the U.S. Department of Energy under Contract No. DE-AC02-05CH11231. We acknowledge the use of the Legacy Archive for Microwave Background Data Analysis (LAMBDA). Support for LAMBDA is provided by the NASA Office of Space Science.

ORCID iDs

Christian L. Reichardt https://orcid.org/0000-0003-2226-9169

References

Abazajian, K. N., Adshead, P., Ahmed, Z., et al. 2016, arXiv:1610.02743
Ade, P. A. R., Aikin, R. W., Barkats, D., et al. 2014, PhRvL, 112, 241101
Ade, P. A. R., Arnold, K., Atlas, M., et al. 2015, PhRvD, 92, 123509
Battaner, E., Florido, E., & Jimenez-Vicente, J. 1997, A&A, 326, 13
Benson, B. A., Ade, P. A. R., Ahmed, Z., et al. 2014, Proc. SPIE, 9153, 91531P
Broderick, A. E., Chang, P., & Pfrommer, C. 2012, ApJ, 752, 22
Carroll, S. M. 1998, PhRvL, 81, 3067
Crites, A. T., Henning, J. W., Ade, P. A. R., et al. 2015, ApJ, 805, 36
Dermer, C. D., Cavadini, M., Razzaque, S., et al. 2011, ApJL, 733, L21
Durrer, R., & Caprini, C. 2003, JCAP, 11, 010
Giovannini, M. 2004, IJMPD, 13, 391
Grasso, D., & Riotto, A. 1998, PhLB, 418, 258
Hanson, D., Hoover, S., Crites, A., et al. 2013, PhRvL, 111, 141301
Henderson, S. W., Allison, R., Austermann, J., et al. 2016, JLTP, 184, 772
Ichiki, K., Takahashi, K., Ohno, H., Hanayama, H., & Sugiyama, N. 2006, Sci, 311, 827
Kahniashvili, T., Lavrelashvili, G., & Ratra, B. 2008, PhRvD, 78, 063012
Kahniashvili, T., Tevzadze, A. G., Sethi, S. K., Pandey, K., & Ratra, B. 2010, PhRvD, 82, 083005
Keck Array and BICEP2 Collaborations, Ade, P. A. R., Ahmed, Z., Aikin, R. W., et al. 2016, PhRvL, 116, 031302
Keisler, R., Hoover, S., Harrington, N., et al. 2015, ApJ, 807, 151
Kesden, M., Cooray, A., & Kamionkowski, M. 2002, PhRvL, 89, 011304
Knox, L. 1997, ApJ, 480, 72
Knox, L., & Song, Y. 2002, PhRvL, 89, 011303

Kosowsky, A., & Loeb, A. 1996, ApJ, 469, 1
Kuehn, K., Lawrence, J., Brown, D. M., et al. 2014, Proc. SPIE, 9147, 914710
Kunze, K. E., & Komatsu, E. 2014, JCAP, 1, 9
Kunze, K. E., & Komatsu, E. 2015, JCAP, 6, 027
Larsen, P., Challinor, A., Sherwin, B. D., & Mak, D. 2016, PhRvL, 117, 151102
Lay, O. P., & Halverson, N. W. 2000, ApJ, 543, 787
Lewis, A. 2004, PhRvD, 70, 043011
Lewis, A., & Bridle, S. 2002, PhRvD, 66, 103511
Lewis, A., Challinor, A., & Lasenby, A. 2000, ApJ, 538, 473
Louis, T., Grace, E., Hasslefield, M., et al. 2016, arXiv:1610.02360
Lue, A., Wang, L., & Kamionkowski, M. 1999, PhRvL, 83, 1506
Mack, A., Kahniashvili, T., & Kosowsky, A. 2002, PhRvD, 65, 123004
Naess, S., Hasselfield, M., McMahon, J., et al. 2014, JCAP, 10, 7
Neronov, A., & Vovk, I. 2010, Sci, 328, 73
Planck Collaboration, Aghanim, N., Arnaud, M., et al. 2016, A&A, 594, A19
Ryu, D., Schleicher, D. R. G., Treumann, R. A., Tsagas, C. G., & Widrow, L. M. 2012, SSRv, 166, 1
Seljak, U., & Hirata, C. M. 2004, PhRvD, 69, 043005
Seshadri, T. R., & Subramanian, K. 2001, PhRvL, 87, 101301
Shaw, J. R., & Lewis, A. 2010, PhRvD, 81, 043517
Simard, G., Hanson, D., & Holder, G. 2015, ApJ, 807, 166
Subramanian, K. 2016, RPPh, 79, 076901
Suzuki, A., Ade, P. A. R., Akiba, Y., et al. 2016, JLTP, 184, 805
Tavecchio, F., Ghisellini, G., Foschini, L., et al. 2010, MNRAS, 406, L70
Taylor, A. M., Vovk, I., & Neronov, A. 2011, A&A, 529, A144
The POLARBEAR Collaboration, Ade, P. A. R., Akiba, Y., Anthony, A. E., et al. 2014, ApJ, 794, 171
Turner, M. S., & Widrow, L. M. 1988, PhRvD, 37, 2743
Vovk, I., Taylor, A. M., Semikoz, D., & Neronov, A. 2012, ApJL, 747, L14
Widrow, L. M., Ryu, D., Schleicher, D. R. G., et al. 2012, SSRv, 166, 37
Wolz, L., Kilbinger, M., Weller, J., & Giannantonio, T. 2012, JCAP, 9, 009
Zucca, A., Li, Y., & Pogosian, L. 2016, arXiv:1611.00757